

Supporting Information

Synergetic spin crossover and fluorescence in a mononuclear iron(III) complex

Table of Contents

Experimental Details

Table S1. Crystallographic data and structural refinements for **1**.

Table S2. Crystallographic data and structural refinements for **2**.

Table S3. Selected structural parameters for **1** and **2**.

Table S4. Hydrogen-bonding interactions for **1** and **2**.

Figure S1. Powder X-ray diffraction (PXRD) patterns for **1** and **2**.

Figure S2 Thermogravimetric analysis (TGA) curves of **1** and **2**.

Figure S3. The first derivative of magnetic susceptibility data of **1**.

Figure S4. The differential scanning calorimetry (DSC) curves at 10 K min⁻¹ for **1**.

Figure S5. Asymmetric unit diagram of **1** at 300 K.

Figure S6. Asymmetric unit diagram of **1** at 120 K.

Figure S7. Asymmetric unit diagram of **2** at 295 K.

Figure S8. Asymmetric unit diagram of **2** at 120 K.

Figure S9. The intermolecular interactions of **1** at 300 K

Figure S10. The intermolecular interactions of **1** at 120 K.

Figure S11. The intermolecular interactions of **2** at 295 K.

Figure S12. The intermolecular interactions of **2** at 120 K.

Figure S13. Variable-temperature fluorescence emission spectra of H₂azp ligand.

Figure S14. Normalized fluorescence emission intensities for H₂azp ligand.

Figure S15. Fluorescence emission spectra of H₂azp ligand in methanol.

Figure S16. Solid-state fluorescence excitation spectrum for **1** at 300 K.

Figure S17. Normalized fluorescence emission intensities for **1**.

Figure S18. Normalized fluorescence emission intensities for **2**.

Figure S19. UV-visible absorption spectra of H₂azp, **1** and **2**.

Experimental Details

Materials and General Methods

All the chemical reagents and solvents were commercially available and used without further purification. The precursor $K[Fe(azp)_2]$ ($H_2azp = 2,2'$ -azodiphenol) was synthesized according to the reported method and dried under vacuum at 80 °C for 5 hours to remove the solvent molecules.¹ The powder X-ray diffraction (PXRD) patterns were obtained on a Rigaku SmartLab X-ray diffractometer (Cu $K\alpha$, $\lambda = 1.54056 \text{ \AA}$) at room temperature. Thermogravimetric analyses (TGA) were carried out on a TG209 F1 Libra under a flowing nitrogen atmosphere at a heating rate of 10 K min^{-1} . Differential scanning calorimetry (DSC) measurement was performed by cooling and heating the crystals in an aluminum crucible using a NETZSCH5 with a sweeping rate of 10 K min^{-1} under nitrogen. The C, H, and N microanalyses were performed on a Elementar Vario-EL CHNS elemental analyzer. FT-IR spectra were recorded in KBr tablets on a Thermo Scientific Nicolet 6700-Continuum instrument in the range of 4000–400 cm^{-1} . UV-vis absorption spectra of liquid samples in the range of 200–800 nm were recorded on a Shimadzu UV-3600 Plus UV-VIS-NIR spectrophotometer equipped with an integrating sphere. The fluorescence spectra for the solid samples in the heating mode were measured on an Edinburgh FL 980 fluorescence spectrophotometer equipped with Xenon lamps and coupled to ARS cryostat.

Synthesis

Synthesis of (FEA) $[Fe(azp)_2] \cdot H_2O$ (1). 6 mL aqueous solution of 2-fluoroethylamine hydrochloride (20 mg, 0.2 mmol) was slowly added to 8 mL methanol/water solution ($V_{MeOH}: V_{H_2O} = 1:1$) of $K[Fe(azp)_2]$ (53 mg, 0.1 mmol) and then stirred for 12 hours. Black microcrystals were collected by filtration, which were further dissolved in methanol/water mixture ($V_{MeOH}: V_{H_2O}=3:2$) and evaporate for one week to afford **1** (37 mg, yield 65%) as black block crystals. Anal. Calcd. for $C_{26}H_{25}FFeN_5O_5$: C, 55.53; H, 4.48; N, 12.45. Found: C, 55.32; H, 4.41; N, 12.50. IR spectra (KBr, cm^{-1}): 3621(w), 3415(br), 2866(br), 1586(s), 1563(m), 1538(m), 1468(s), 1447(w), 1370(m), 1288(s), 1243(m), 1140(s), 1002(w), 843(m), 751(s), 612(m), 526(m).

Synthesis of (CIEA) $[Fe(azp)_2] \cdot H_2O$ (2). Compound **2** was synthesized by a similar method to compound **1**. 2-Chloroethylamine hydrochloride (23mg, 0.2 mmol) was used. Black block crystals of **2** (29 mg, yield 50%) were collected. Anal. Calcd. for $C_{26}H_{25}ClFeN_5O_5$: C, 53.95; H, 4.35; N, 12.10. Found: C, 53.77; H, 4.50; N, 12.07. IR spectra (KBr, cm^{-1}): 3627(w), 3402(br), 2850(br), 1590(s), 1563(m), 1539(m), 1467(s), 1447(w), 1375(m), 1324(m), 1288(s), 1247(s), 1211(w), 1140(s), 1027(w), 940(w), 843(s), 751(s), 612(m), 520(s).

Magnetic measurements

Magnetic susceptibility measurements were performed on a Quantum Design PPMS3 SQUID magnetometer with a sweep rate of 2 K min^{-1} under an applied field of 5 kOe. Data were corrected for the signal of the sample holder and diamagnetic contribution calculated from Pascal's constants.

Single crystal X-ray diffraction

Variable temperature single crystal X-ray diffraction data of **1** at 120 and 300 K and **2** at 295 K were performed with Bruker D8 QUEST diffractometer with Mo $K\alpha$ ($\lambda = 0.71073 \text{ \AA}$) radiation, respectively. The data indexing and integration processes were performed using Bruker Smart program. Single-crystal X-ray crystallographic data of **2** was collected on a Rigaku XtaLAB

Synergy Custom diffractometer with a CCD area detector (Cu K α radiation, $\lambda = 1.54184 \text{ \AA}$) at 120 K. The data reduction was carried out with the CrysAlisPro SuperNova system program. The structures were solved by direct methods using SHELXTL crystallographic software package.² All non-hydrogen atoms were refined with anisotropic displacement parameters by least squares on weighted F^2 values in OLEX 2.³ The hydrogen atoms were constrained to idealized geometries by using a riding model. The crystallographic data are deposited in the Cambridge Crystallographic Data Centre (CCDC). The CCDC numbers are 2386139, 2386140, 2386141 and 2390175.

Table S1. Crystallographic data and structural refinements for **1**.

Parameter	1	
	120	300
Chemical Formula	C ₂₆ H ₂₅ FFeN ₅ O ₅	
Mr	562.36	
Crystal system	triclinic	triclinic
Space group	$\bar{p}1$	$\bar{p}1$
<i>a</i> /Å	10.2719(6)	10.3263(5)
<i>b</i> /Å	11.2960(7)	11.7230(6)
<i>c</i> /Å	12.0615(7)	12.4752(6)
α /°	68.508(2)	66.229(2)
β /°	65.942(2)	65.108(2)
γ /°	81.917(2)	81.559(2)
<i>V</i> /Å ³	1189.02(12)	1253.20(11)
<i>Z</i>	2	2
$\rho_{\text{calcd.}}$ (g/cm ³)	1.571	1.490
μ (mm ⁻¹)	0.692	0.657
F(000)	582.0	582.0
Radiation	Mo K α (λ = 0.71073)	Mo K α (λ = 0.71073)
Reflections collected	29375	24099
Independent reflections	5491	5441
Goodness-of-fit on F ²	1.054	1.076
Final <i>R</i> indexes [<i>I</i> >= 2 σ (<i>I</i>)] ^a	<i>R</i> ₁ = 0.0407, <i>wR</i> ₂ = 0.0895	<i>R</i> ₁ = 0.0338, <i>wR</i> ₂ = 0.0864
Final <i>R</i> indexes [all data]	<i>R</i> ₁ = 0.0590, <i>wR</i> ₂ = 0.0971	<i>R</i> ₁ = 0.0413, <i>wR</i> ₂ = 0.0911
Largest diff. peak/hole / e Å ⁻³	0.58/-0.78	0.28/-0.41
CCDC No.	2386139	2386140

^a $R_1 = \Sigma ||F_o| - |F_c|| / \Sigma |F_o|$; $wR_2 = \{[\Sigma w(F_o^2 - F_c^2)^2] / \Sigma [w(F_o^2)^2]\}^{1/2}$.

Table S2. Crystallographic data and structural refinements for **2**.

Parameter	2	
	120	295
Chemical Formula	C ₂₆ H ₂₅ ClFeN ₅ O ₅	
Mr	578.81	
Crystal system	triclinic	triclinic
Space group	$\bar{P}1$	$\bar{P}1$
<i>a</i> /Å	10.1942(3)	10.306(2)
<i>b</i> /Å	12.1461(3)	12.235(3)
<i>c</i> /Å	12.1213(4)	12.191(3)
α /°	66.188(3)	66.110(7)
β /°	65.374(3)	65.439(8)
γ /°	83.184(2)	82.870(7)
<i>V</i> /Å ³	1245.99(7)	1276.5(5)
<i>Z</i>	2	2
$\rho_{\text{calcd.}}$ (g/cm ³)	1.543	1.506
μ (mm ⁻¹)	6.257	0.743
F(000)	598.0	598.0
Radiation	Cu K α (λ = 1.54184)	Mo K α (λ = 0.71073)
Reflections collected	11351	19889
Independent reflections	4886	4566
Goodness-of-fit on <i>F</i> ²	1.029	1.064
Final <i>R</i> indexes [<i>I</i> >= 2 σ (<i>I</i>)] ^a	<i>R</i> ₁ = 0.0461, <i>wR</i> ₂ = 0.1241	<i>R</i> ₁ = 0.0693, <i>wR</i> ₂ = 0.1691
Final <i>R</i> indexes [all data]	<i>R</i> ₁ = 0.0474, <i>wR</i> ₂ = 0.1252	<i>R</i> ₁ = 0.1178, <i>wR</i> ₂ = 0.1953
Largest diff. peak/hole / e Å ⁻³	1.09/-0.91	0.83/-0.59
CCDC No.	2386141	2390175

^a $R_1 = \Sigma ||F_o| - |F_c|| / \Sigma |F_o|$; $wR_2 = \{[\Sigma w(F_o^2 - F_c^2)^2] / \Sigma [w(F_o^2)^2]\}^{1/2}$.

Table S3. Selected structural parameters for **1** and **2**.

Parameter	1 (300 K)	1 (120 K)	2 (295 K)	2 (120 K)
Fe1–N2	2.1475(14)	1.9239(17)	2.144(4)	2.1340(2)
Fe1–N3	2.1522(14)	1.9124(17)	2.149(4)	2.1503(19)
<Fe–N> ^a	2.1499(14)	1.9182(17)	2.147(4)	2.1422(11)
Fe1–O1	1.9715(12)	1.8952(15)	1.964(3)	1.9712(17)
Fe1–O2	2.0052(13)	1.9234(15)	1.983(4)	1.9928(18)
Fe1–O3	2.0114(13)	1.9523(15)	2.012(3)	2.0076(16)
Fe1–O4	1.9160(13)	1.8562(15)	1.914(4)	1.9237(17)
<Fe–O> ^b	1.9760(13)	1.9068(15)	1.968(4)	1.9738(17)
\sum Fe ^c	92.9	45.1	90.8	88.7
$\pi\cdots\pi$ ^d	3.632(16)	3.532(17)	3.711(5)	3.662(2)

^aThe average Fe–N bond lengths (Å); ^bThe average Fe–O bond lengths (Å); ^cOctahedral distortion parameter (°);

^dThe distance between the centroid of benzene rings (C19–C24) in the unit of Å.

Table S4. Hydrogen-bonding interactions for **1** and **2**.

Parameter	<i>D</i> -H... <i>A</i>	<i>D</i> -H (Å)	H... <i>A</i> (Å)	<i>D</i> ... <i>A</i> (Å)	<i>D</i> -H... <i>A</i> (°)
1 (300 K)	O5-H5D...O2	0.85	2.15	2.832(3)	137.0
	N5-H5A...O3 ^{#2}	0.89	2.01	2.848(2)	156.1
	N5-H5B...O5	0.89	1.90	2.790(3)	176.0
	N5-H5B...O5A	0.89	1.82	2.618(6)	148.3
	N5-H5C...O1 ^{#2}	0.89	1.97	2.847(2)	167.4
	O5A-H5AA...O2	0.85	1.85	2.667(6)	161.5
1 (120 K)	O5-H5D...O2	0.87	2.18	2.814(2)	129.6
	N5-H5A...O3 ^{#1}	0.91	1.96	2.826(2)	158.7
	N5-H5B...O5	0.91	1.85	2.764(2)	179.7
	N5-H5C...O1 ^{#2}	0.91	1.96	2.861(2)	169.9
	C2-H2...F1 ^{#3}	0.95	2.60	3.487(3)	154.9
	C11-H11...O2 ^{#1}	0.95	2.57	3.459(3)	156.2
2 (295 K)	O5-H5D...O2	0.85	1.96	2.802(7)	171.5
	N5-H5A...O3 ^{#1}	0.89	1.98	2.810(5)	153.7
	N5-H5B...O5	0.89	1.87	2.750(7)	170.3
	N5-H5B...O5A	0.89	1.76	2.590(18)	154.7
	N5-H5C...O1 ^{#2}	0.89	1.97	2.856(5)	174.7
	O5A-H5AA...O2	0.85	1.76	2.564(18)	156.1
	O5A-H5AB...O3 ^{#1}	0.85	2.66	3.420(2)	149.9
	C26-H26B...O5	0.97	2.66	3.341(10)	127.9
2 (120 K)	O5-H5D...O2	0.85	2.12	2.718(3)	127.5
	N5-H5A...O3 ^{#2}	0.91	1.96	2.811(2)	155.7
	N5-H5B...O5	0.91	1.83	2.738(3)	173.7
	N5-H5C...O1 ^{#2}	0.91	1.92	2.827(3)	175.0
	C26-H26B...O5	0.99	2.60	3.281(3)	125.7

Symmetry codes: #1: 1-X,1-Y,1-Z; #2: -1+X,+Y,+Z; #3: 1+X,+Y,+Z.

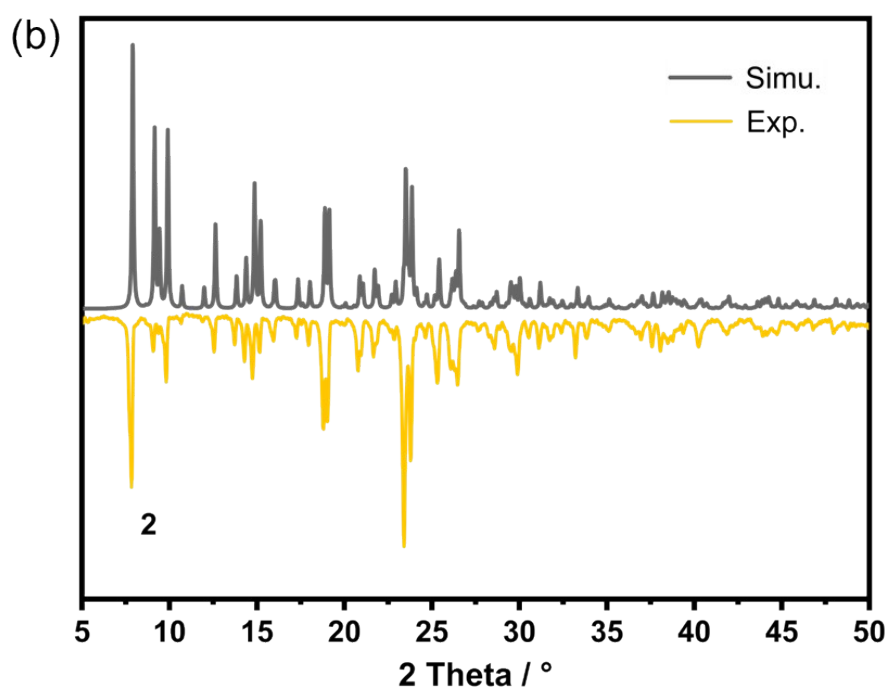
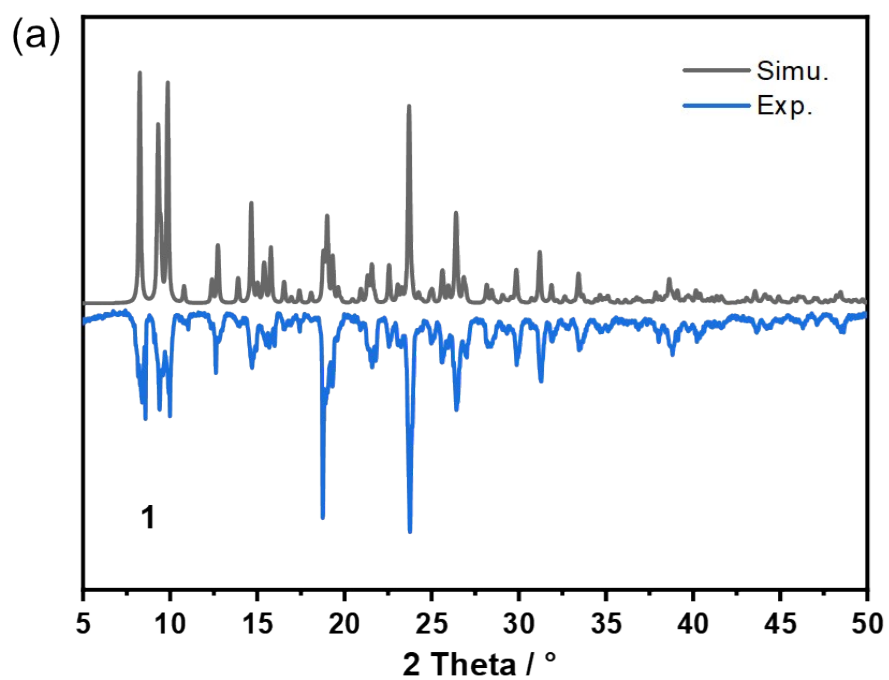


Figure S1. Powder X-ray diffraction (PXRD) patterns for **1** (a) and **2** (b). The simulated PXRD patterns for **1** and **2** were obtained by using crystal data at 300 and 295 K, respectively.

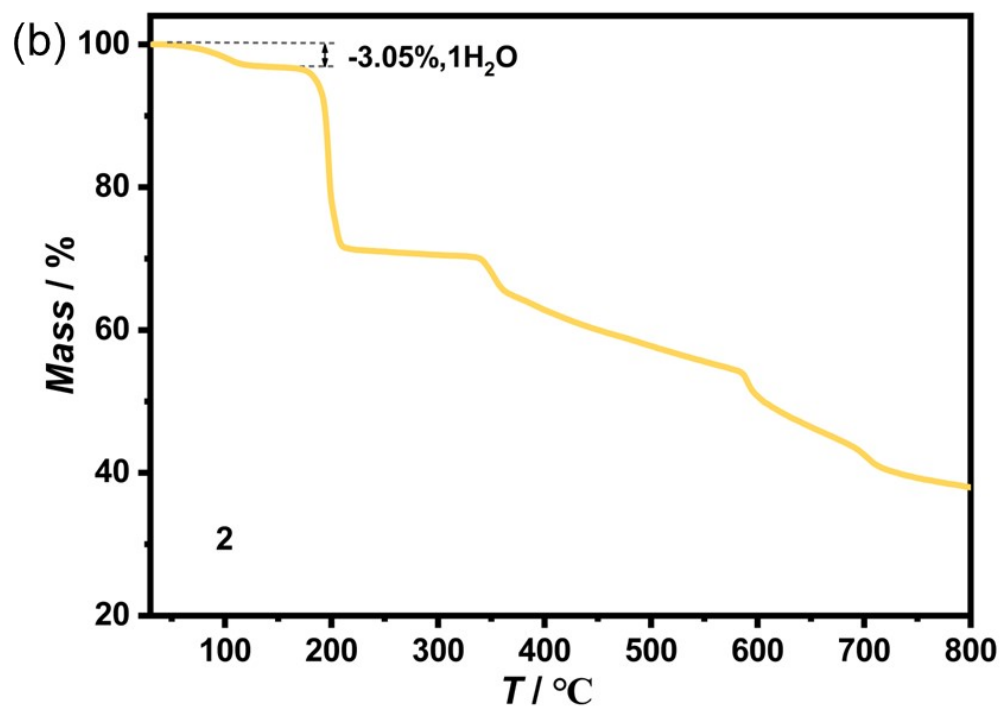
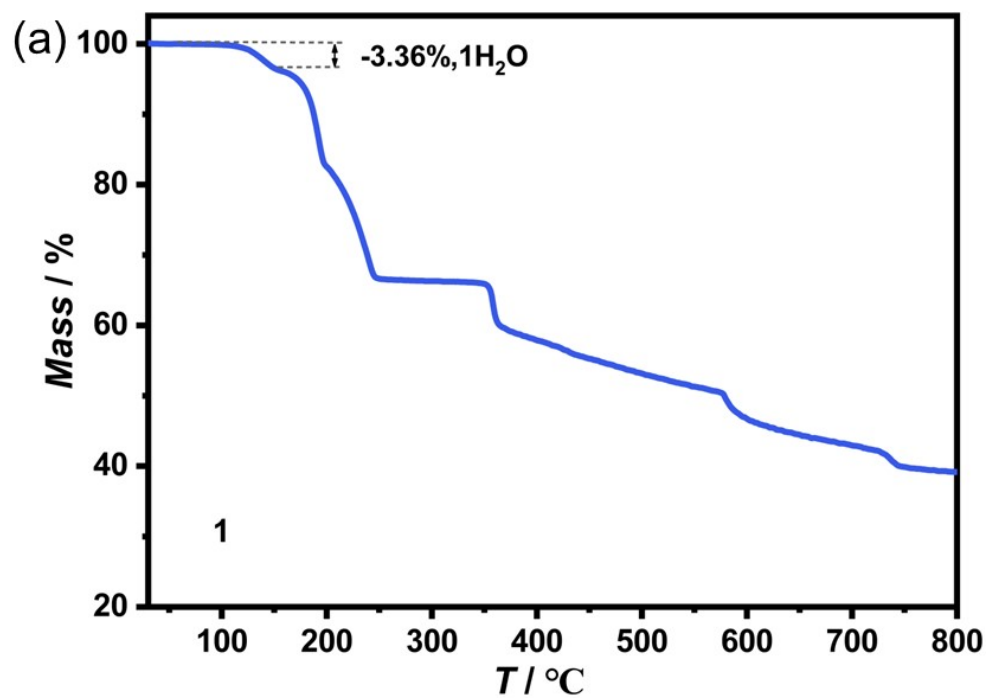


Figure S2. Thermogravimetric analysis (TGA) curves of **1** (a) and **2** (b). The weight loss of 3.36% and 3.05% are close to the theoretical values of 3.20% and 3.11% corresponding to the escape of one water molecule in **1** and **2**, respectively.

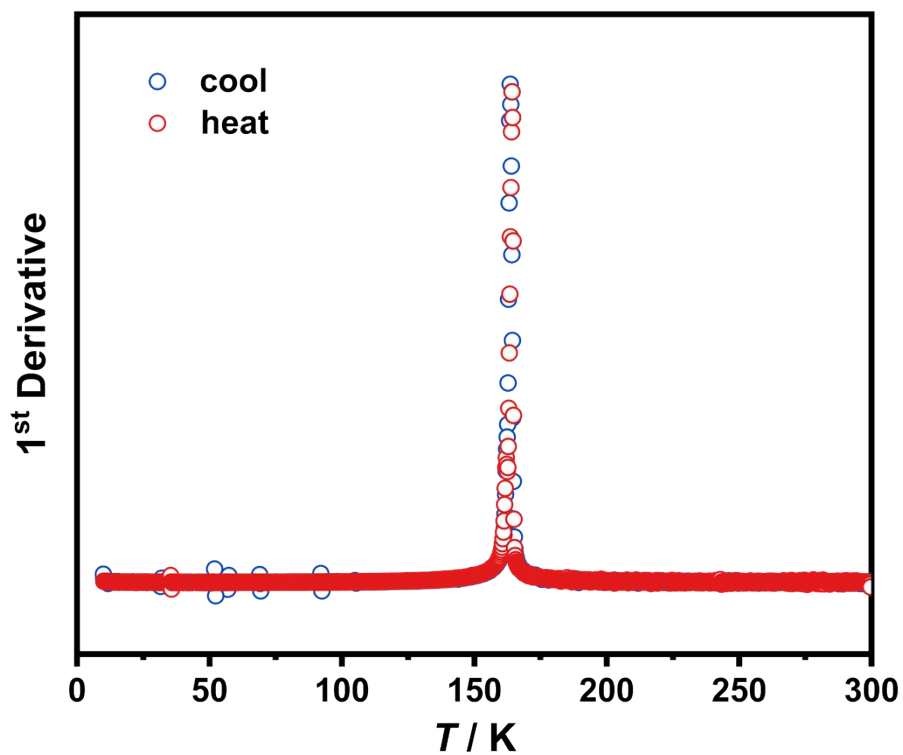


Figure S3. The first derivative of magnetic susceptibility data of **1**.

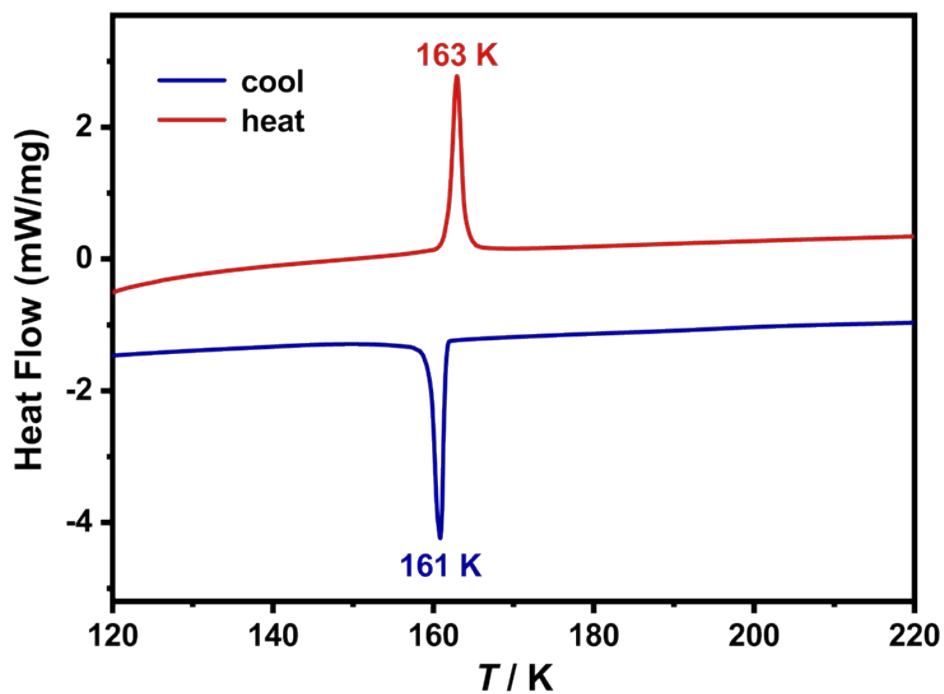


Figure S4. The differential scanning calorimetry (DSC) curves at 10 K min^{-1} for **1** in the cooling (blue) and heating (red) modes.

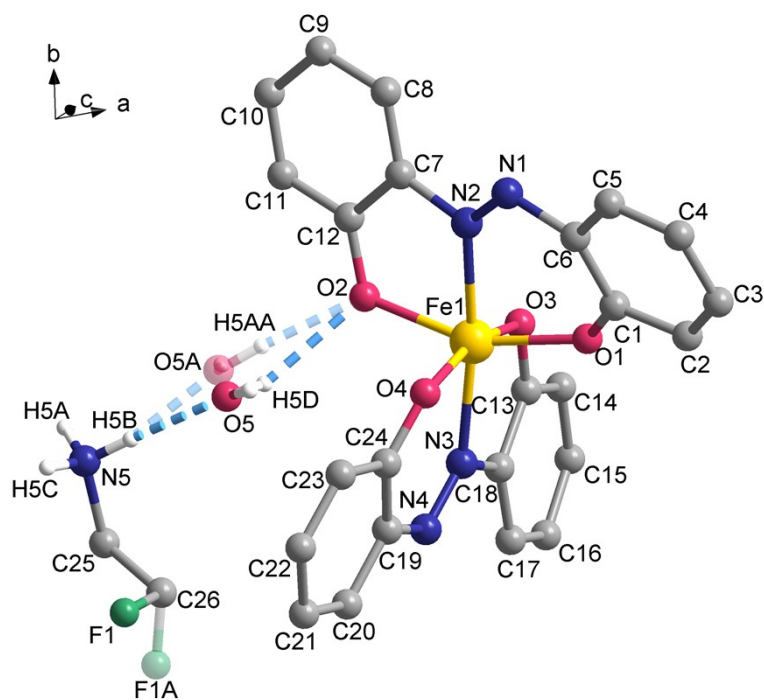


Figure S5. Asymmetric unit of **1** at 300 K. Color codes: Fe, yellow; C, gray; N, blue; O, red; F, green. The F1 and O5 are disordered over two positions with a ratio of 85:15 and 75:25, respectively. Only the hydrogen atoms on N5 and O5 are shown.

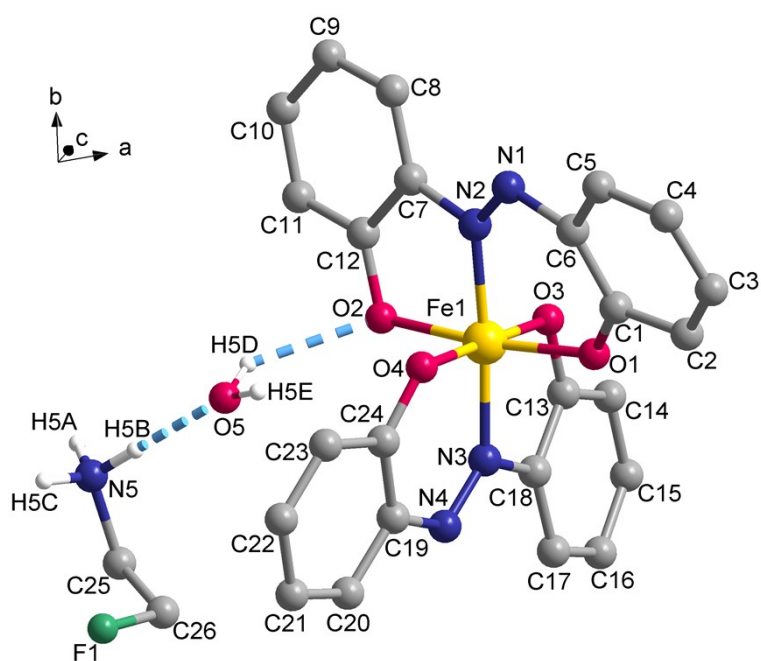


Figure S6. Asymmetric unit diagram of **1** at 120 K. Color codes: Fe, yellow; C, gray; N, blue; O, red; F, green. Only the hydrogen atoms on N5 and O5 are shown.

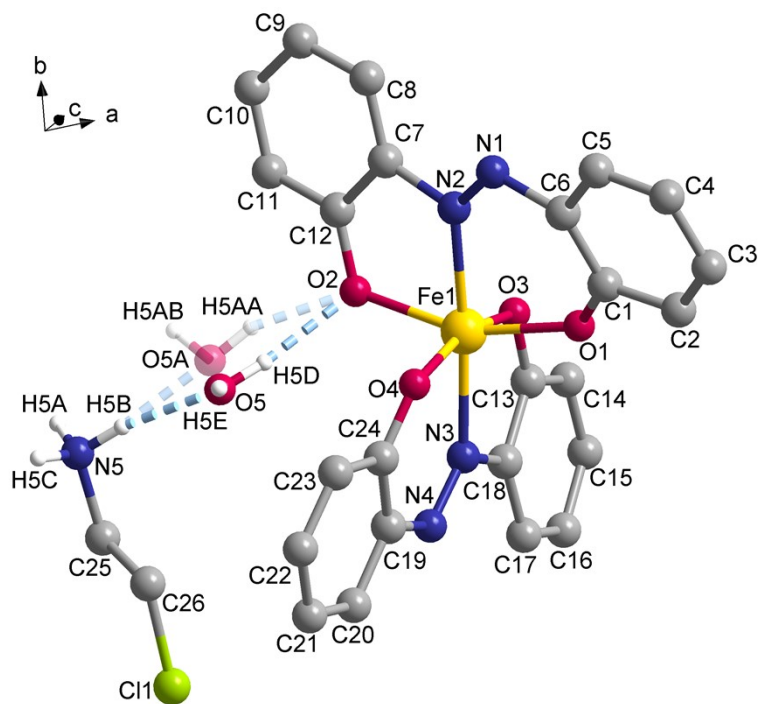


Figure S7. Asymmetric unit diagram of **2** at 295 K. Color codes: Fe, yellow; C, gray; N, blue; O, red; Cl, green. Only the hydrogen atoms on N5 and O5 are shown.

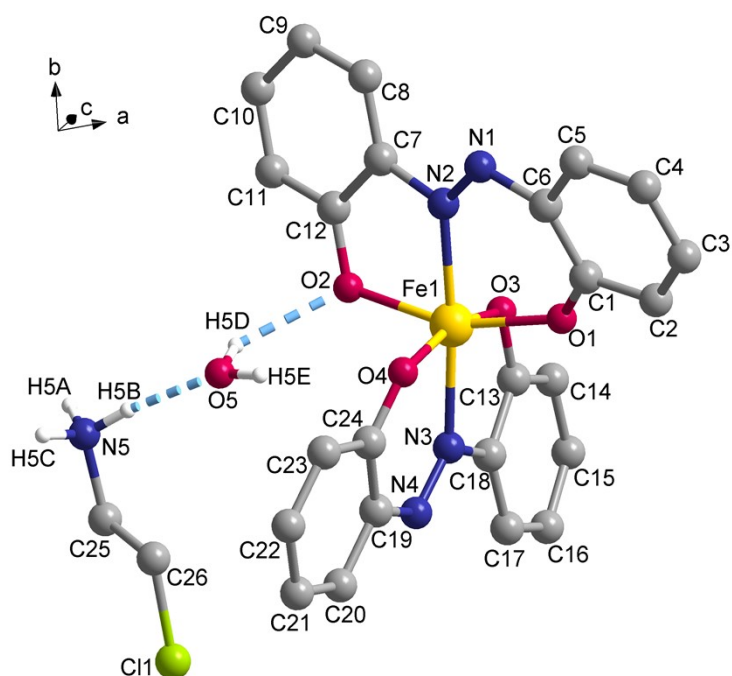


Figure S8. Asymmetric unit diagram of **2** at 120 K. Color code: Fe, yellow; C, gray; N, blue; O, red; Cl, green. Only the hydrogen atoms on N5 and O5 are shown.

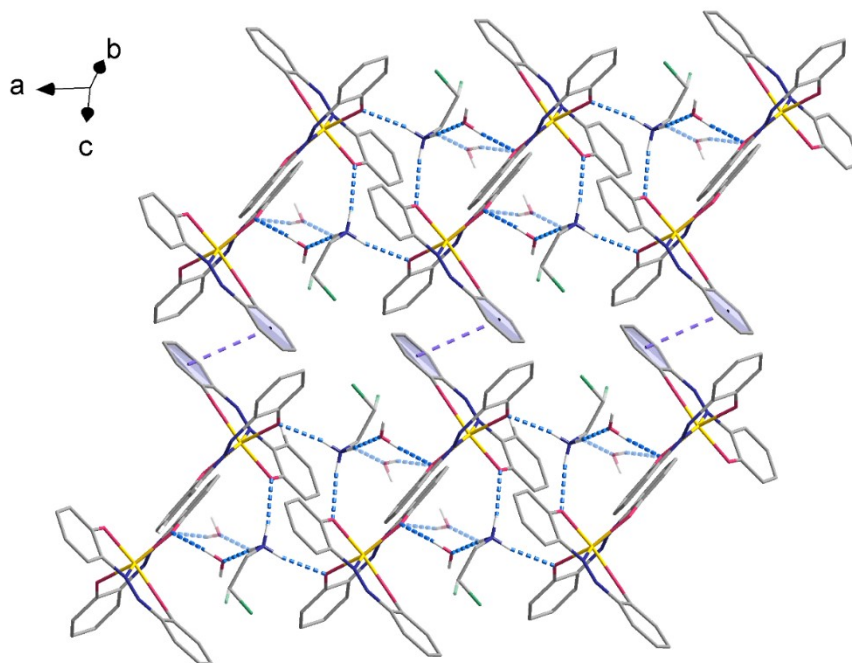


Figure S9. The intermolecular interactions of **1** at 300K: N–H \cdots O (blue dashed lines), O5–H5D \cdots O2 (blue dashed lines), offset face-to-face $\pi\cdots\pi$ interactions (purple dashed lines).

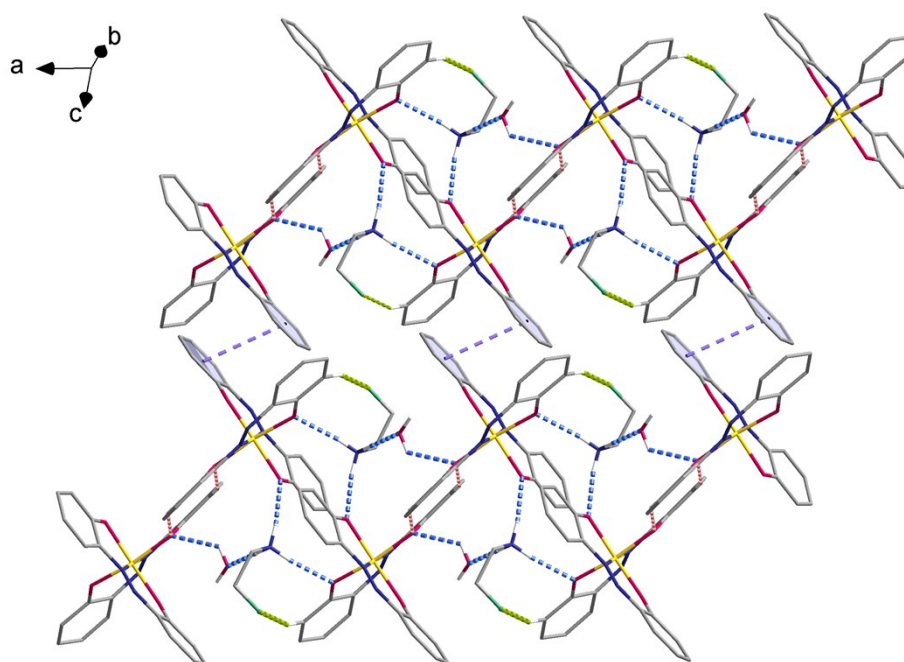


Figure S10. The intermolecular interactions of **1** at 120 K: N–H \cdots O (blue dashed lines), O5–H5D \cdots O2 (blue dashed lines), offset face-to-face $\pi\cdots\pi$ interactions (purple dashed lines), C11–H11 \cdots O2 (pink dashed lines) and C2–H2 \cdots F1 (green dashed lines).

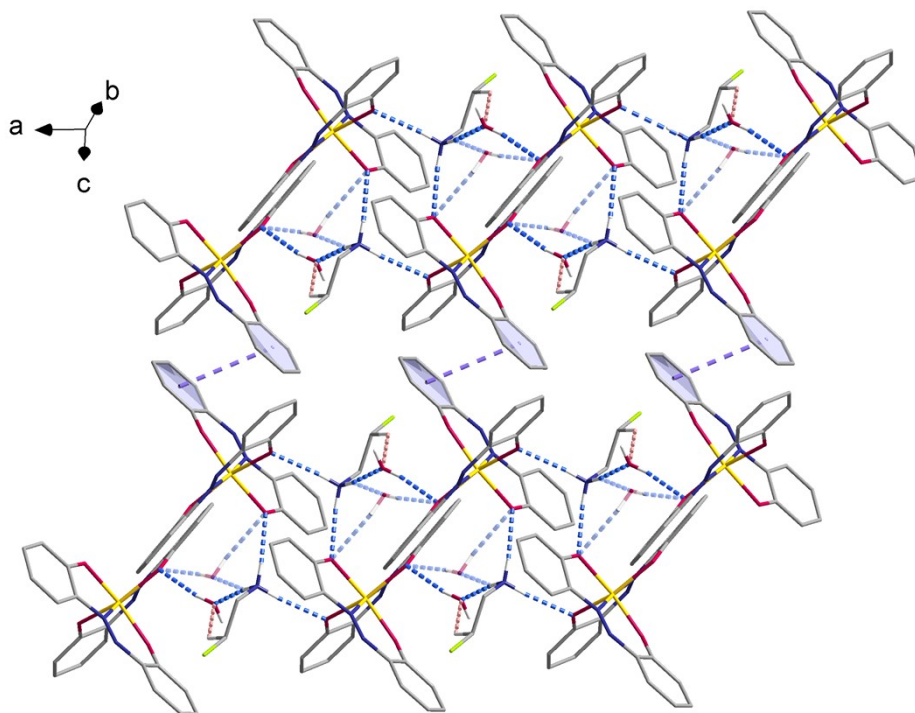


Figure S11. The intermolecular interactions of **2** at 295 K: N-H...O (blue dashed lines), O-H...O (blue dashed lines), offset face-to-face π ... π interactions (purple dashed lines), C26-H26B...O5 (pink dashed lines).

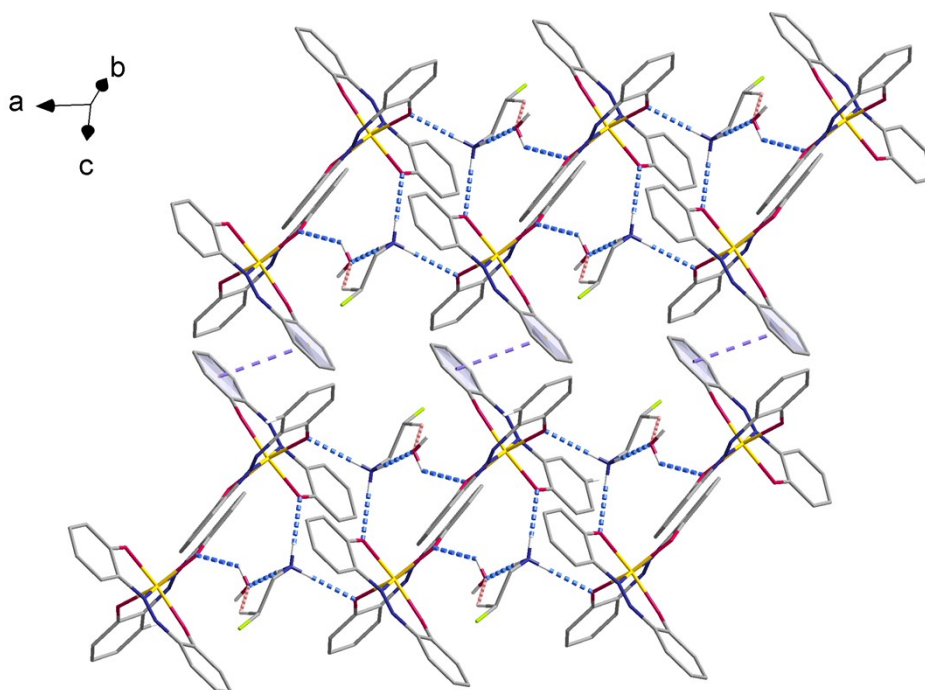


Figure S12. The intermolecular interactions of **2** at 120 K: N-H...O (blue dashed lines), O5-H5D...O2 (blue dashed lines), offset face-to-face π ... π interactions (purple dashed lines), C26-H26B...O5 (pink dashed lines).

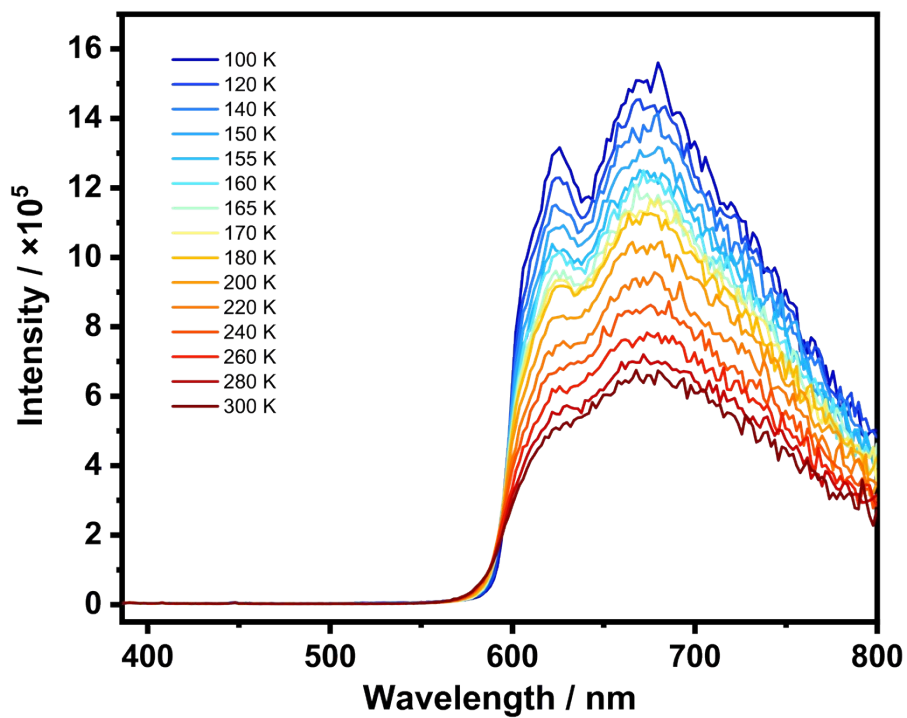


Figure S13. Variable-temperature fluorescence emission spectra of H₂azp ligand ($\lambda_{\text{ex}} = 348$ nm) from 100 to 300 K.

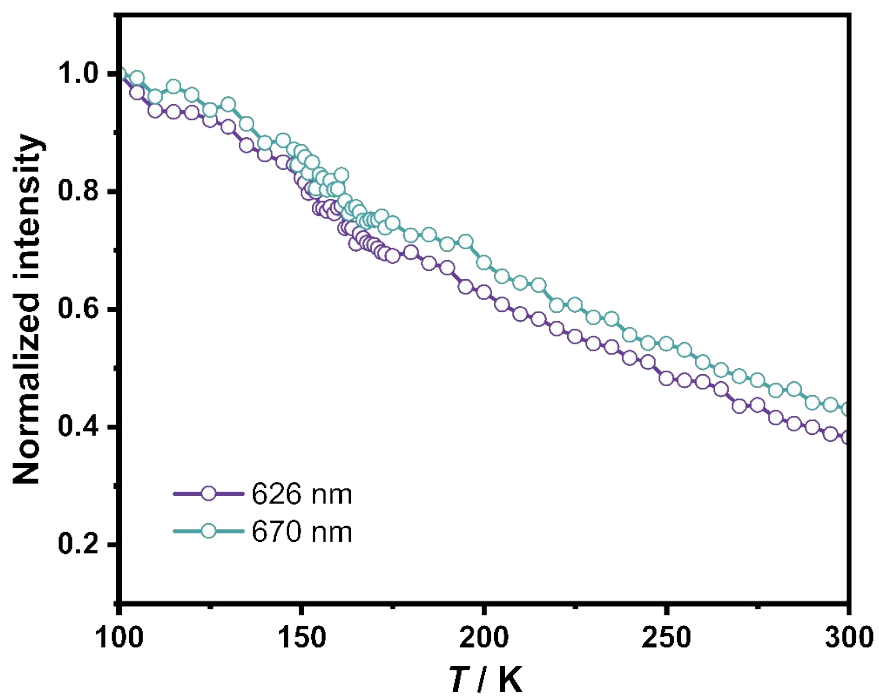


Fig. S14. Normalized fluorescence emission intensities at 626 and 670 nm for H₂azp ligand.

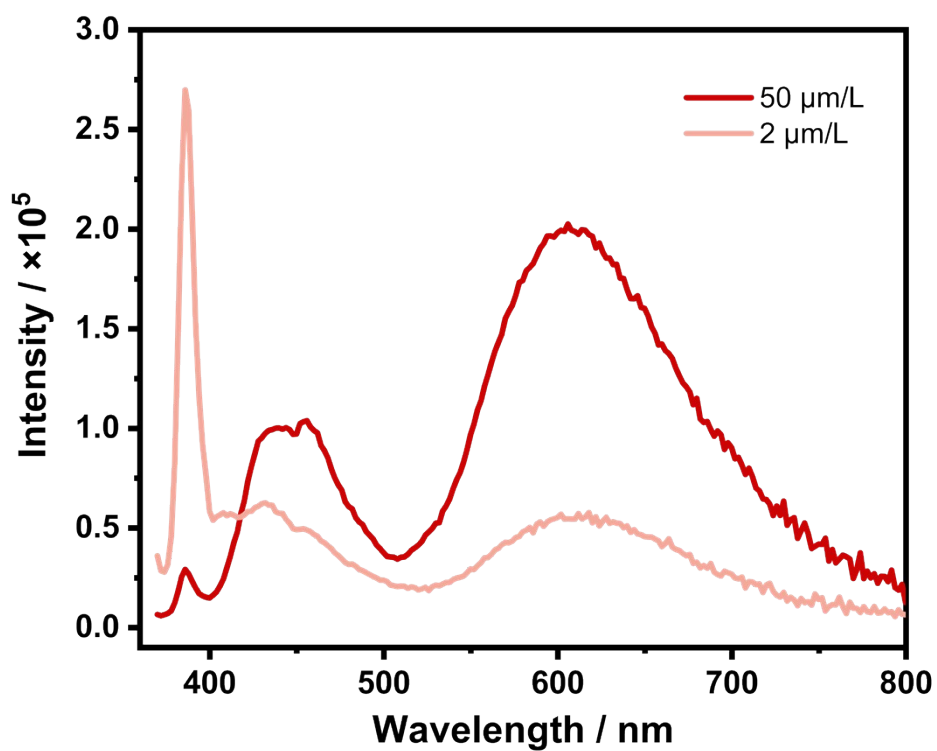


Fig. S15. Fluorescence emission spectra of H₂azp ligand in methanol ($\lambda_{\text{ex}} = 348 \text{ nm}$).

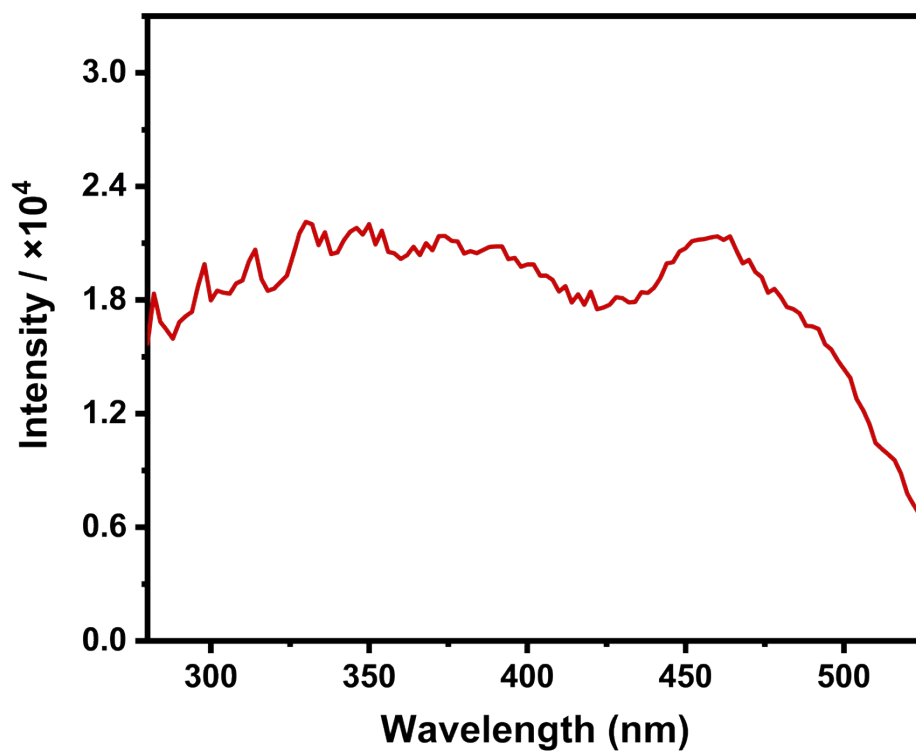


Figure S16. Solid-state fluorescence excitation spectrum monitored at 664 nm for 1 at 300 K.

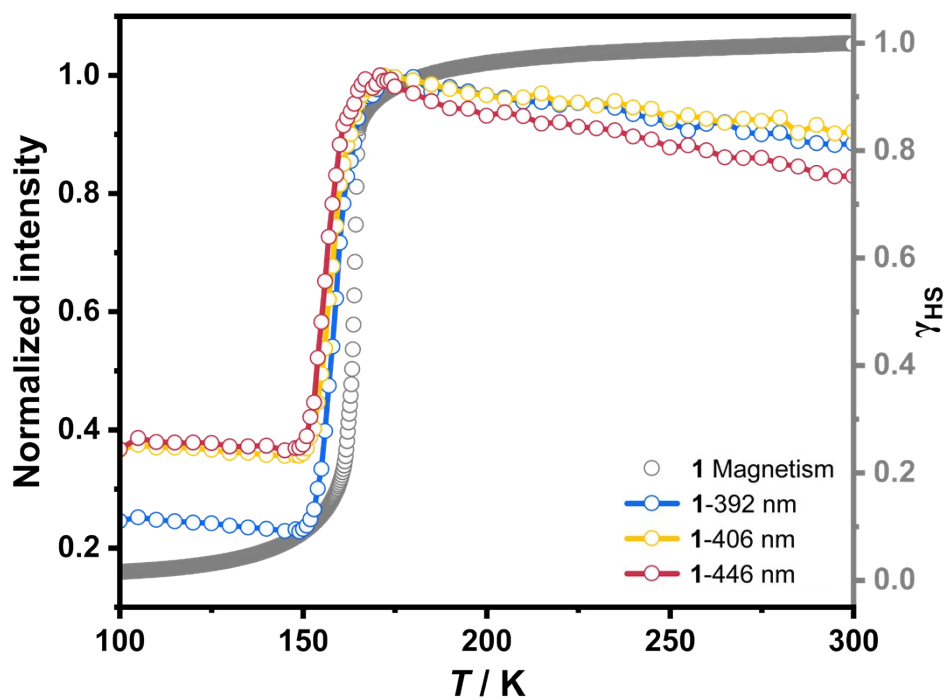


Fig. S17. Normalized fluorescence emission intensities at 392, 406 and 446 nm for **1** ($\lambda_{\text{ex}} = 348$ nm).

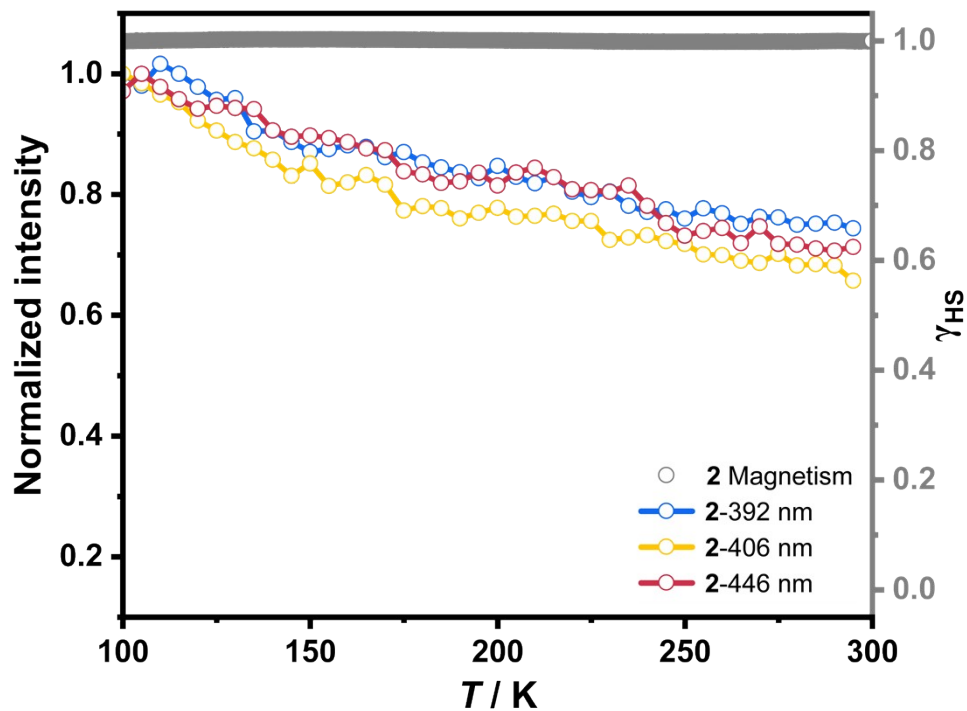


Fig. S18. Normalized fluorescence emission intensities at 392, 406 and 446 nm for **2** ($\lambda_{\text{ex}} = 348$ nm).

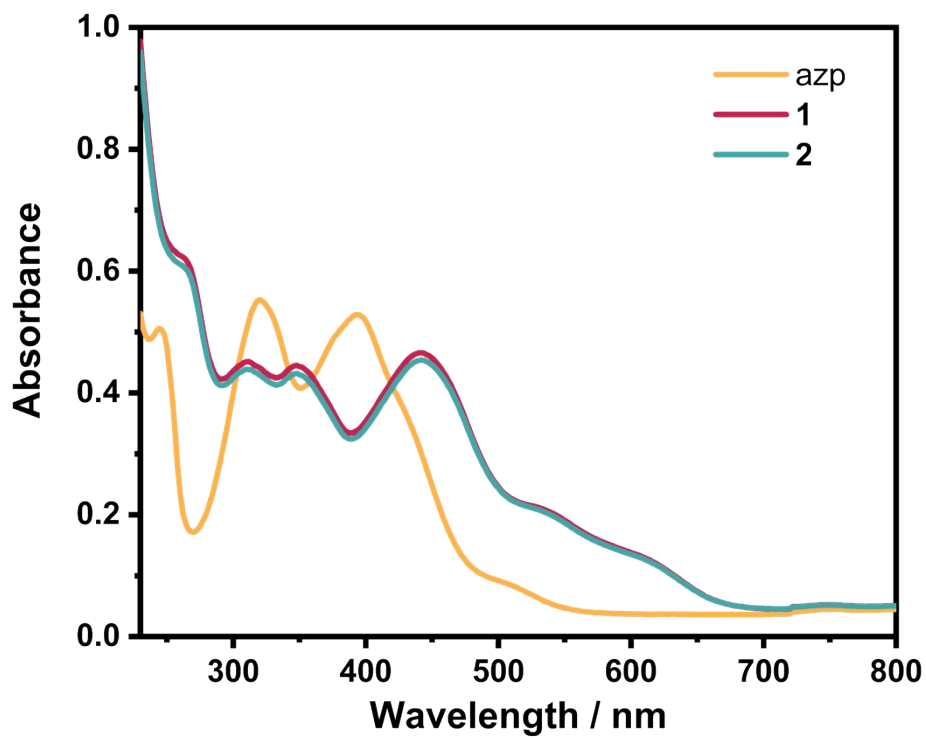


Figure S19. UV-visible absorption spectra of H₂azp, **1** and **2** in methanol solution (1 μM /L) at room temperature.

References

- 1 K. Takahashi, K. Kawamukai, M. Okai, T. Mochida, T. Sakurai, H. Ohta, T. Yamamoto, Y. Einaga, Y. Shiota and K. Yoshizawa, *Chem. Eur. J.*, 2015, **22**, 1253–1257.
- 2 (a) G. M. Sheldrick, SHELXS-97, Program for Crystal Structure solution. University of Göttingen, Germany 1997. (b) G. M. Sheldrick, SHELXL-97, Program for Crystal Structure Refinement. University of Göttingen, Germany 1997. (c) G. M. Sheldrick, Crystal structure refinement with SHELXL. *Acta Crystallogr. C* 2015, **71**, 3–8.
- 3 O. V. Dolomanov, L. J. Bourhis, R. J. Gildea, J. A. K. Howard and H. Puschmann, OLEX2: a complete structure solution, refinement and analysis program, *J. Appl. Crystallogr.*, 2009, **42**, 339–341.